Publication Year	2009
Acceptance in OA@INAF	2023-02-08T10:51:56Z
Title	Planck LFI CPV: TSA Failure and Thermal Dynamic Response
Authors	TERENZI, LUCA; Tomasi, Maurizio; FRAILIS, Marco; FRANCESCHI, ENRICO; GALEOTTA, Samuele; et al.
Handle	http://hdl.handle.net/20.500.12386/33272
Number	PL-LFI-PST-RP-078

UniMi – UniTs – INAF/OATs – IASF-BO – IBO – ESA – Univ. Helsinki
LFI Project System Team

Planck LFI

TITLE: **Planck LFI CPV: TSA Failure and Thermal Dynamic Response (ref: P_PVP_LFI_0023_01)**

DOC. TYPE: Test Report
PROJECT REF.: PL-LFI-PST-RP-078 **PAGE:** I of IV, 12
ISSUE/REV.: 1.1 **DATE:** **09 Oct, 2009**

Prepared by	**L. Terenzi** **M. Tomasi** **M. Frailis** **E. Franceschi** **S. Galeotta** **D. Tavagnacco** **A. Zacchei** **G. Morgante** **D. Pearson** **F. Cuttaia** **A. Gregorio** **A. Mennella** **P. Battaglia** **M. Bersanelli** **R. Davis** **A. De Rosa** **C. Franceschet** **R. Leonardi** **S. Lowe** **R. Mandolesi** **M. Maris** **P. Meinhold** **L. Mendes** **T. Poutanen** **M. Sandri** **L. Valenziano** **F. Villa** **A. Wilkinson** **A. Zonca**	**Date:**	October , 2009
	Signature:	

		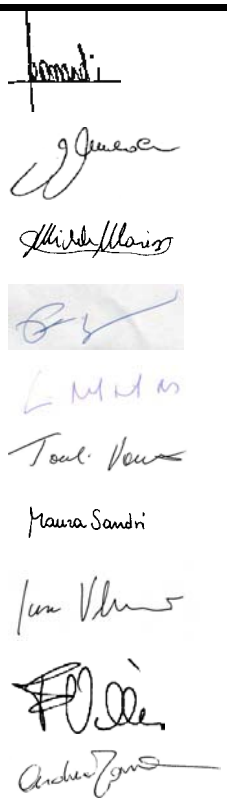
Agreed by	**C. BUTLER** **LFI Program Manager**	**Date:** October , 2009 **Signature:** 
Approved by	**N. MANDOLESI** **LFI Principal Investigator**	**Date:** October , 2009 **Signature:** 

The Planck-LFI calibration team

- Paola Battaglia (SCOS/TQL operator)
- Marco Bersanelli (LFI instrument scientist, test leader)
- Francesco Cuttaia (CPV responsible, test leader, data analysis)
- Richard Davis (30/44 GHz data analysis)
- A. De Rosa (SCOS/TQL operator)
- Marco Frailis (Level 1 manager)
- Cristian Franceschet (SCOS/TQL operator)
- Enrico Franceschi (GSE manager)
- Samuele Galeotta (LIFE/PEGASO development)
- Anna Gregorio (Instrument Operation Manager)
- Rodrigo Leonardi (data analysis)
- Stuart Lowe (LIFE/PEGASO development)
- Reno Mandolesi (Principal Investigator)
- Michele Maris (data analysis, LIFE/PEGASO development)
- Peter Meinhold (Test leader, data analysis)
- Luis Mendes (data analysis)
- Aniello Mennella (Calibration Scientist, test leader, data analysis)
- Gianluca Morgante (SCS support to LFI)
- Dave Pearson (SCS support to LFI)
- Torsti Poutanen (data analysis)
- Maura Sandri (Test leader, data analysis)
- Daniele Tavagnacco (SCOS/TQL operator)
- Luca Terenzi (Tests leader, data analysis and LIFE/PEGASO development)
- Maurizio Tomasi (Test leader, data analysis and LIFE/PEGASO development)
- Luca Valenziano (SCOS/TQL operator)
- Fabrizio Villa (Test leader, data analysis)
- Althea Wilkinson (30/44 GHz data analysis)
- Andrea Zacchei (LFI DPC manager)
- Andrea Zonca (SCOS/TQL operator, LIFE/PEGASO development)

DISTRIBUTION LIST

Recipient	Company / Institute	E-mail address	Sent
M. BERSANELLI	UNIMI – Milano	marco.bersanelli@mi.infn.it	Yes
R.C. BUTLER	INAF/IASF – Bologna	butler@iasfbo.inaf.it	Yes
F. CUTTAIA	INAF/IASF – Bologna	cuttaia@iasfbo.inaf.it	Yes
A. GREGORIO	UniTs – Trieste	Anna.gregorio@ts.infn.it	Yes
N. MANDOLESI	INAF/IASF – Bologna	mandolesi@iasfbo.inaf.it	Yes
A. MENNELLA	UNIMI – Milano	aniello.mennella@fisica.unimi.it	Yes
A. ZACCHEI	INAF/OATs – Trieste	zacchei@oats.inaf.it	Yes
LFI Core team coordinators		lfi_ctc@iasfbo.inaf.it	Yes
LFI radiometer core team		planck_cta02@fisica.unimi.it	Yes
LFI calibration team			
LFI System PCC	INAF/IASF – Bologna	lfispcc@iasfbo.inaf.it	Yes

CHANGE RECORD

Issue	Date	Sheet	Description of Change	Release

TABLE OF CONTENTS

1 ACRONYMS

AIV	Assembly, Integration, Verification
ASW	Application Software
BEM	Back End Module
BEU	Back End Unit
CCS	Central Check-out System
CDMU	Central Data Management Unit
DAE	Data Acquisition Electronics
DPU	Digital Processing Unit
EGSE	Electrical ground Support Equipment
FEM	Front End Module
FPU	Focal Plane Unit
I-EGSE	Instrument EGSE
IST	Integrated Satellite Test
OBC	On Board Clock
RAA	Radiometer Array Assembly
REBA	Radiometric Electronic Box Assembly
S/C	Spacecraft
SCOE	Spacecraft Control and Operation System
SPU	Signal Processing Unit
SUSW	Start- Up Software
SVM	Service Module
TBC	To Be Checked
TBW	To Be Written
TC	Telecommand
TM	Telemetry
UFT	Unit Functional Test

2 APPLICABLE AND REFERENCE DOCUMENTS

2.1 Applicable Documents

[AD1] Herschel/Planck Instrument Interface document Part A, SCI-PT-IIDA-04624 Issue 3.3

[AD2] Herschel/Planck Instrument Interface document Part B, SCI-PT-IIDB-04142 Issue 3.1

[AD3] Herschel/Planck Instrument Interface document Part B, SCI-PT-IIDB-04142 Issue 3.1, Annex 3, ICD 750800115

[AD4] Herschel/Planck Instrument Interface document Part A, SCI-PT-IIDA-04624 Issue 3.3 Annex 10

[AD5] Data analysis and scientific performance of the LFI FM instrument, PL-LFI-PST-AN-006 3.0

[AD6] Planck-LFI TV-TB test report: executive summary, PL-LFI-PST-RP-040 1.1

2.2 Reference Documents

[RD1] Planck Instrument Testing at PFM S/C levels, H-P-3-ASP-TN-0676, Issue 1.0

[RD2] Planck LFI User Manual, PL-LFI-PST-MA-001 Issue 2.1

[RD3] M.Tomasi et al., Dynamic Validation of the Planck/LFI Thermal Model, 2009, submitted to JINST

3 INTRODUCTION

3.1 Purpose and Scope

Characterize the dynamic behaviour of the LFI Focal Plane with no active control of the TSA temperature, evaluate transfer functions between FPU sensors and compare results with previous tests and thermal model predictions.

3.2 Test configuration

The test configuration is the following

SCOS 2 K HPCCS Version 2.0.787
LFI Gateway Version V0R9P1
TQL 3.1.2
LIFE Machine version OM 3.00

Personnel involved during the test is:

LFI Instrument Operation Manager	Anna Gregorio UniTs anna.gregorio@ts.infn.it
LFI Calibration Scientist	Aniello Mennella UniMi aniello.mennella@fisica.unimi.it
LFI CPV Manager	Francesco Cuttaia INAF – IASF Bologna cuttaia@iasfbo.inaf.it
Test leader	L. Terenzi
LFI IOT	Enrico Franceschi, Marco Frailis, Samuele Galeotta, Andrea Zacchei, Maurizio Tomasi, Daniele Tavagnacco
SCS IOT	G. Morgante, D. Pearson
Industry support	

4 Test Execution

4.1 Pass-fail criteria, verification matrix

CPV P_PVP_LFI_0023_01
July, 29 2009 OD 77
Duration 24 hours
Test name: TSA failure and thermal dynamic response

Test objectives: Characterise the dynamic behaviour of Thermal Model and susceptibility.

Verification matrix

Check	Passed?			Recovered?	
	Yes	No	Notes	Yes	No
No unexpected events packets	Yes				
Housekeeping and Science production telemetry as expected	Yes				
Test sequence succesfully run		No	Duration was agreed to be reduced to 4 hours. Data are enough for the analysis to be run.	Yes	
Real time data available	Yes				
Data saved and stored at DPC	Yes				

The test was run succesfully. A reduced duration of the TSA switch off time was agreed before the test started.

4.2 Procedure/ Test sequence

The test started on July 29th at 6:00 UTC when the sorption cooler TSA was switched off.
The test was run after a steady period of 12 hours when the instruments were working in nominal conditions, so that the comparison between the TSA on nominal setup and the TSA off is also possible as an additional information for the thermal susceptibility test.
The duration of 4 hours was agreed in order to have a sufficient number of cooler cycle monitored and at the same time to minimize the time the system is kept out of the nominal state, so to avoid other cryochain parts than LFI FPU interface to be affected.
On July 29th at 10:00 UTC the TSA was activated back.
An overview of relevant temperature data are given in Fig. 2, where also the FPU temperature steady state period before the test is visible. An overview of the FPU sensors is given in Fig. 1.
The Sorption Cooler nominal unit cold end is located on the bottom right of the figure. After switching off the TSA fluctuation propagates from the TSA to the other sensors location following the direction upwards left.

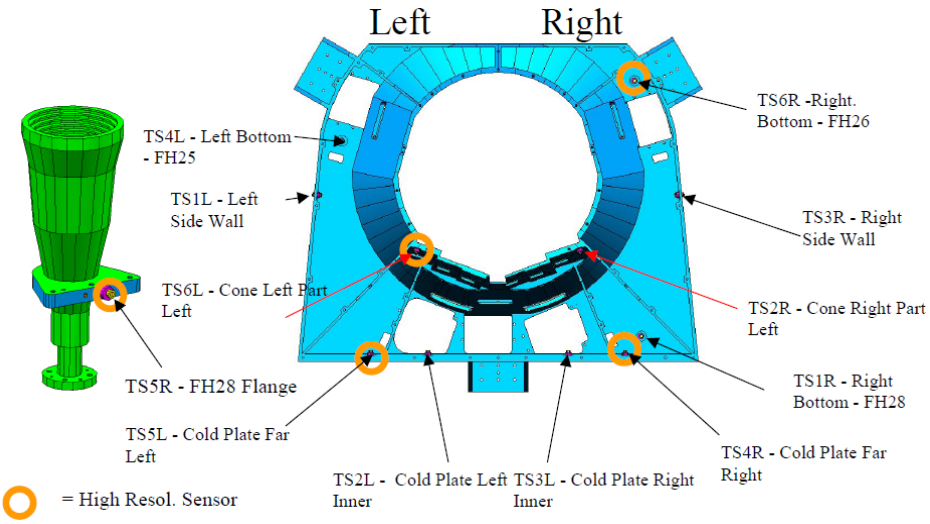

Fig. 1 Temperature sensors location on the LFI focal plane. The cold end interface is in the corner on the bottom right of the figure

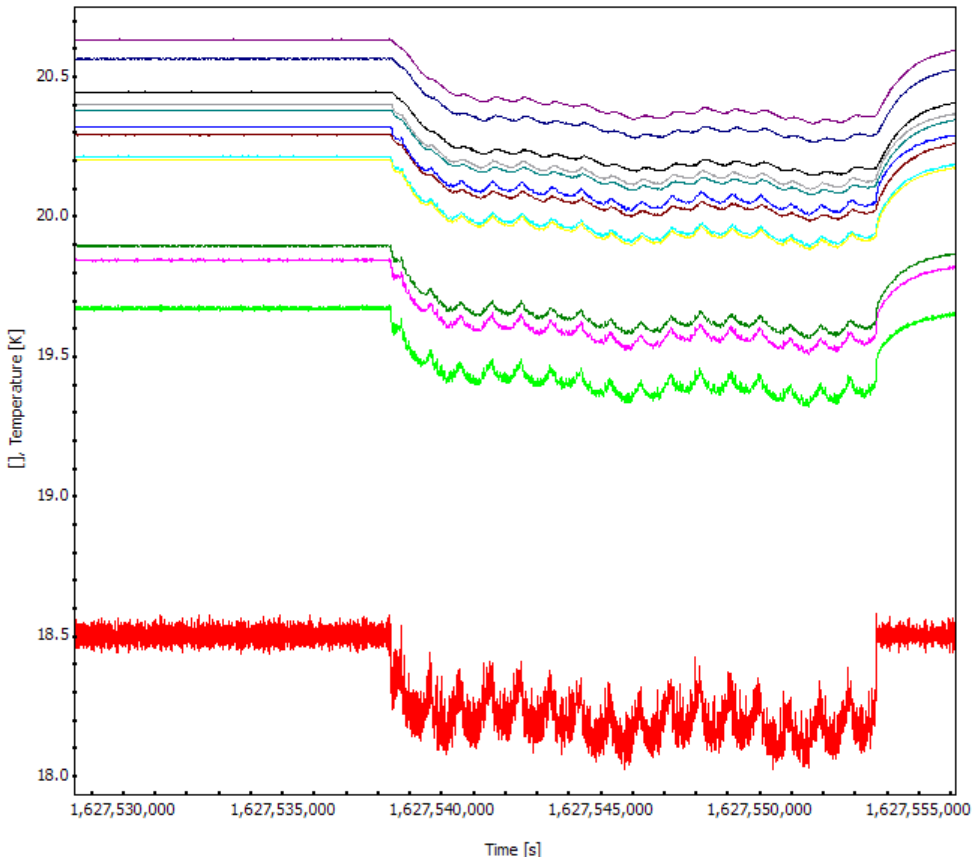

Fig. 2 Temperature sensor curves during the thermal dynamic response test. The red curve is the sorption cooler TSA sensor.

5 Data Analysis

The source of fluctuations is characterized by two main periods which are the sorption cooler typical periods:

1. the bed cycle time, which is set to 940 sec during the test
2. the complete cooler period which is six times larger: 5640 sec in our case.

The first analysis to run is to evaluate the transfer functions of the fluctuation in the TSA temperature to the 12 FPU temperature sensors at the two main frequencies.
Two methods for evaluating the transfer functions were used, as described also in [RD3].
The first method consists on performing a DFT of the sensor timestreams and than evaluating the ratio of the amplitude and the difference of the phases found at the relevant frequencies of interest.
The second method consists in fitting the sensor timestreams with a double sin function:

$$T(t) = T_0 + A_1 \sin(\omega_1 t + \phi_1) + A_2 \sin(\omega_2 t + \phi_2)$$

where $\omega_1 = 1/940$ Hz and $\omega_2 = 1/5640$ Hz: and then transfer functions are evaluated by the ratio of the amplitudes and phases found.

5.1 Tranfer functions from DFT

The total time with steady conditions we can exploit for analysis makes us have a clear DFT for the peak around 1 mHz only, as evident, from the Fig. 3.

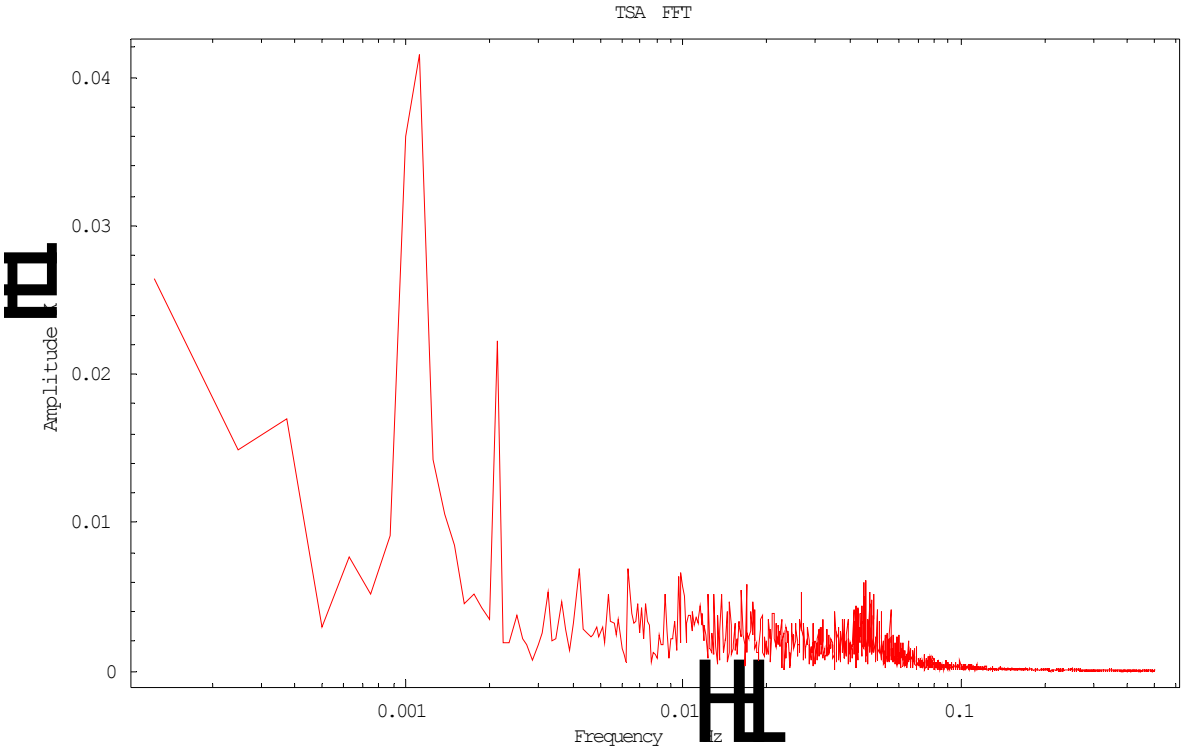

Fig. 3 TSA temeprature DFT during latest test phase (about 8000 sec) before switchng it on again. Peak at 1mHz is evident, while lowerfrequencies are poorly scanned.

So the final results were obtained from points at 0.998 mHz and 1.12 mHz, which are the frequencies closest to the 940sec period fluctuation, which was not resolved exactly by the transform as evident also from Fig. 4.

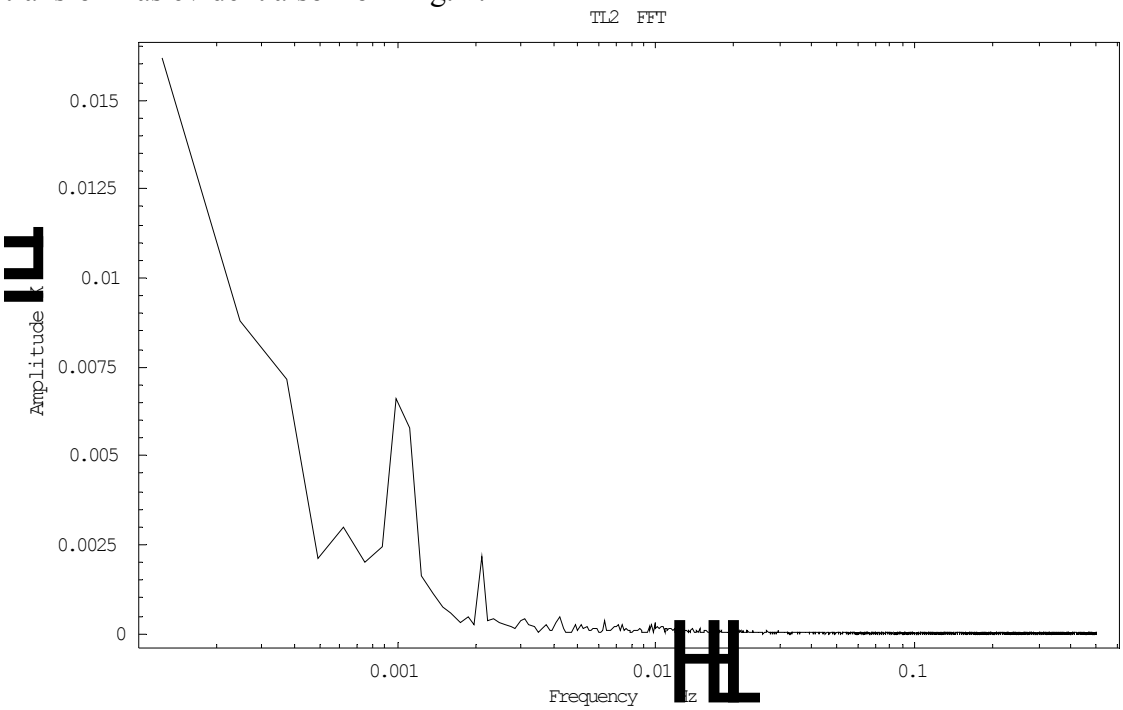

Fig. 4 Discrete fourier transform for the sensor TSL2. the distance between the two points at about 1mHz shows the frequency resolution close to the peak.

The transfer function amplitude is evaluated by the ratio of the amplitudes of the FPU sensors to the TSA one (see
Fig. 5).
The phase is given by the difference between the FPU sensors phase and the TSA sensor phase.

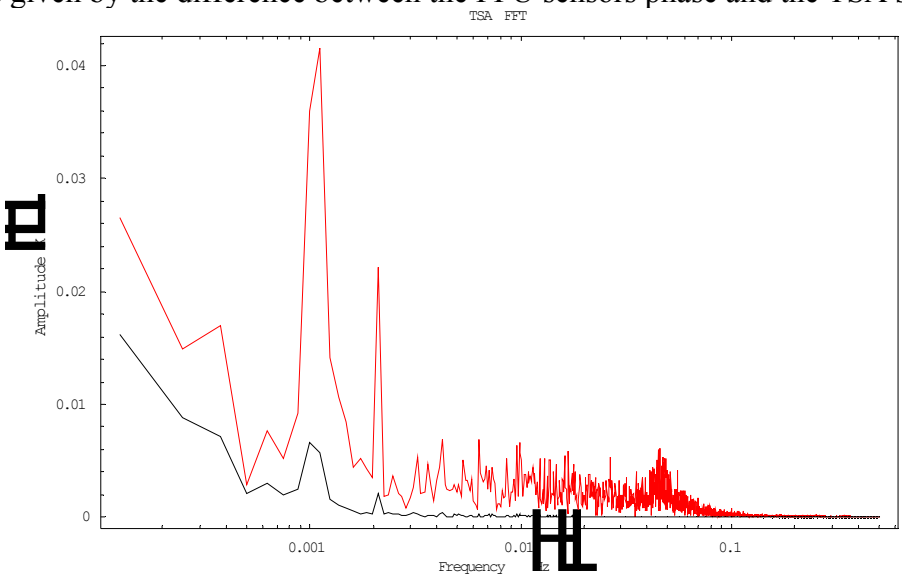

Fig. 5 The TSA Fourier transform amplitude (red) plotted with the TSL2 one (black). The transfer function amplitude is evaluates from the ratio of the two.

Results are shown in Table 1.

	0.998 mHz		1.12 mHz	
Sensor ID	***TF Amp***	***Phase (rad)***	***TF Amp***	***Phase (rad)***
TSL1	0.132	1.58	0.113	1.99
TSL2	0.184	1.09	0.139	1.21
TSL3	0.289	0.64	0.253	0.60
TSL4	0.130	1.60	0.113	2.04
TSL5	0.164	1.27	0.125	1.50
TSL6	0.136	1.51	0.112	1.91
TSR1	0.417	0.36	0.393	0.32
TSR2	0.244	0.88	0.205	0.88
TSR3	0.250	0.86	0.209	0.85
TSR4	0.333	0.53	0.302	0.48
TSR5	0.253	0.86	0.210	0.85
TSR6	0.184	1.17	0.146	1.32

Table 1 Results from DFT analysis for transfer fiunctions of FPU temperature sensors

5.2 Tranfer functions from sinusoidal function fitting

The second method is implemented in the time domain. It consists in fitting as mentioned above each sensor curve with a double sinusoidal function.

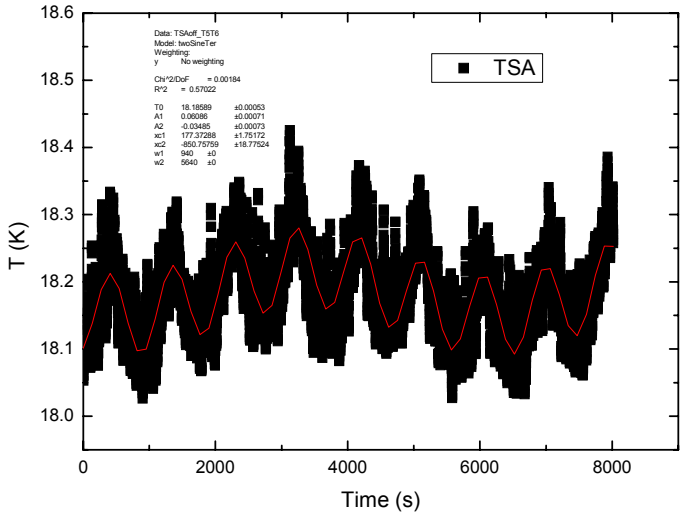

Fig. 6 TSA sensor temperature curve (black points) fitted by a double sinusoidal function (red line).

In Fig. 6, the temperature curve of the TSA sensor is shown together with its fitting curve. The fit is very good also because the TSA sensor is the most variable and it is rapidly decreasing its temperature to the minimum steady state. When fitting the FPU sensors, we realized that a slow drift was occurring again for some of them, in particular the farthest from the cold end temperature sink, so that the simple fit used before was not sufficient to have a detailed data analysis result.

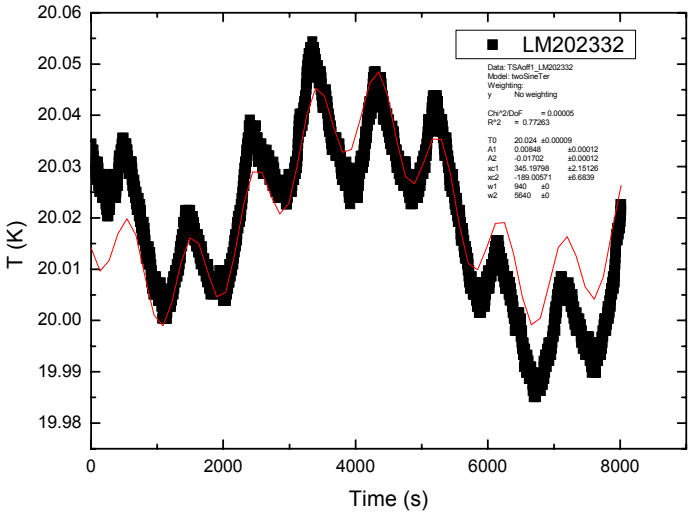

Fig. 7 Temperature curve of the TS2L sensor (black points), plotted together with the double sinusoidal fitting function (red line). A drift is still present in the data and it could affect the quality of the results.

So a further additional exponential decay was added to the fitting function in order to take into account the residual drift and have a compliant fit result (see)

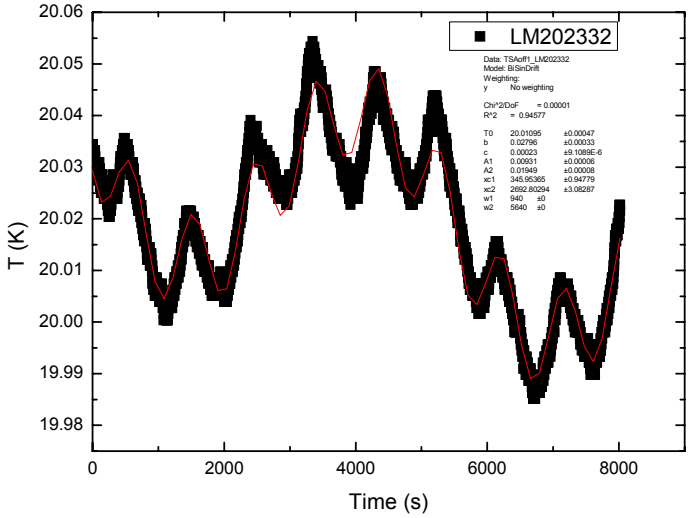

Fig. 8 Temperature curve of the TS2L sensor (black points), plotted together with the new double sinusoidal fitting function with exponential decay (red line).

The final function was defined as:

$$T(t) = T_0 + Be^{-Ct} \; A_1 \sin(\omega_1 t + \phi_1) + A_2 \sin(\omega_2 t + \phi_2)$$

Also in this case the transfer function amplitude is defined by the ratio of the amplitudes of the fit and phases are defined by the differences.
In this last case also the long period component at 5640 sec is monitored in the analysis.
Results are given in Table 2.

	1.064 mHz		**0.177 mHz**	
Sensor ID	***TF Amp***	***Phase (rad)***	***TF Amp***	***Phase (rad)***
TSL1	0.113	1.79	0.520	0.95
TSL2	0.153	1.13	0.560	0.81
TSL3	0.266	0.60	0.600	0.60
TSL4	0.112	1.83	0.522	0.96
TSL5	0.136	1.37	0.554	0.87
TSL6	0.110	1.70	0.483	0.98
TSR1	0.402	0.33	0.660	0.41
TSR2	0.218	0.86	0.583	0.68
TSR3	0.222	0.84	0.589	0.68
TSR4	0.313	0.49	0.616	0.52
TSR5	0.224	0.84	0.586	0.68
TSR6	0.158	1.23	0.545	0.81

Table 2 Results for transfer functions evaluated from the double sinusoidal function fitting with exponential decay.

6 Steady state temperature distribution

A dedicated time, with all temperatures in the focal plane were in a steady condition was allocated since August 2nd 12:00z to August 3rd 12:00z. The corresponding temperature curves of the TSA and FPU sensors are reported in Fig. 9.
In the Table below main statistics (average temperature, standard deviation and peak-to-peak amplitude) for the sensors temperature curve during the 24 hours duration of the test are reported. The TSA was controlled at 18.5 K. The mean value of the peak-to-peak amplitude of the high resolution sensors is of about 4 mK, while the sensor closest to the source of fluctuations and fixed directly on the RCA28 feed horn flange has a p-p amplitude of 4.7 mK, with a reduction of the TSA fluctuations of a factor 45.

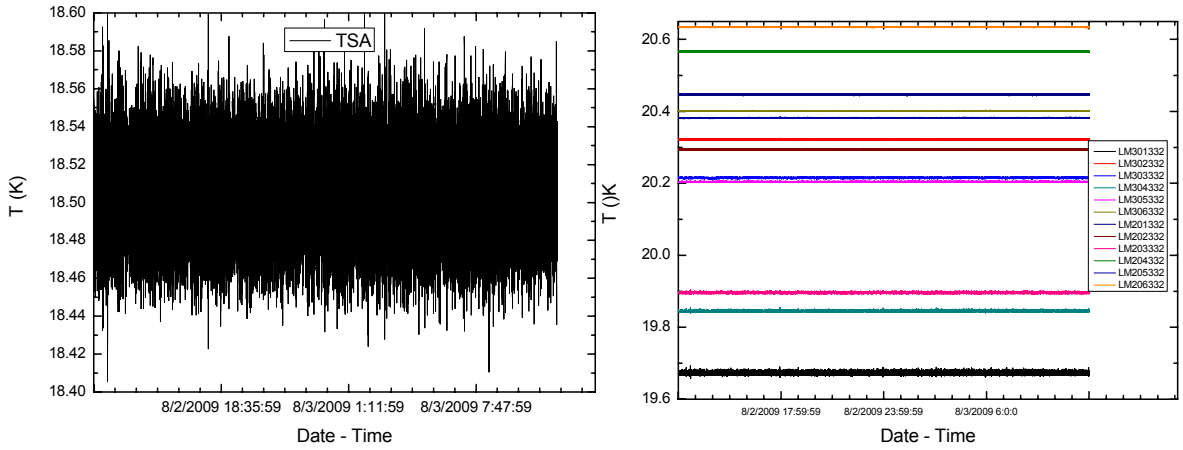

Fig. 9 Steady state temperature curves of the TSA (left panel) and FPU (right panel) sensors

Sensor Id	Mean T (K)	ΔT rms (K)	ΔT p-p (K)
TSA	18.50059	0.02311	0.21227
TSL1	20.44637	7.04331E-4	0.00669
TSL2	20.29393	8.10118E-4	0.00667
TSL3	19.89597	0.00128	0.01176
TSL4	20.56603	7.73461E-4	0.00554
TSL5	20.38185	5.00818E-4	0.004
TSL6	20.63433	5.03124E-4	0.00401
TSR1	19.67198	0.00344	0.03553
TSR2	20.32162	8.91561E-4	0.00667
TSR3	20.21499	8.63764E-4	0.00777
TSR4	19.84482	0.00145	0.0154
TSR5	20.20399	5.85881E-4	0.00467
TSR6	20.40109	5.14072E-4	0.004

7 Conclusions and recommendations

The analysis carried out provides the reference values of in flight transfer functions.
The two methods give a good agreeement when comparing the 1.12 mHz results in Table 1 to the 1.064 mHz results in Table 2.
As expected also the temperatures of the FPU sensors are sorted with ascending values in the direction from the bottom right of the FPU to the upper left side, in a coherent way with fluctuation decrease.
These results then also give a clear view of the heat flux lines through the whole front end unit and main frame.